15-state R-matrix investigation of resonances in elastic scattering of electrons from atomic hydrogen at low energies

W. C. Fon and K. Ratnavelu
Department of Mathematics, University of Malaya, 59100 Kuala Lumpur, Malaysia

K. M. Aggarwal*
Department of Applied Mathematics and Theoretical Physics, The Queen's University of Belfast, Belfast, BT7 1NN, Northern Ireland

(Received 23 October 1992)

A 15-state R-matrix calculation has been carried out at 685 energies ranging from 1–17 eV to depict the resonant profiles for the elastic differential cross sections and the angular distribution of the spin asymmetry $A_{1s\text{-}1s}(\theta,k^2)$ in the elastic scattering of spin-polarized electrons by spin-polarized hydrogen atoms at angles of 30°, 55°, 70°, and 90°. The calculations are compared with experiments.

PACS number(s): 34.80.Bm, 34.80.Nz

I. INTRODUCTION

In general, electron-atom scattering experiments that are performed with unpolarized incident beams and that lack either any polarization analysis or, in the case of reactive collisions, any electron-photon or electron-electron coincidence analysis result in the determination of differential and total cross sections which are averaged over spin and angular-momentum states. The experimental data so derived necessitate some form of normalization procedures before direct comparison can be made with collision theory. It is important, in the investigation of a large number of spin-dependent processes that occur in physics, to have electrons available in well-defined spin states. Thus one is not obliged to average over all possibilities that may arise from different spin directions, thereby losing valuable information. Instead one can investigate the individual possibilities separately.

The development of improved polarized electron sources and of a source of spin-polarized hydrogen atoms has led to the first measurements of the asymmetry between spin-parallel and spin-antiparallel scattering in this fundamental system. The first reported measurements (Alguard *et al.* [1], Wainwright *et al.* [2], Fletcher *et al.* [3], Gay *et al.* [4], and Fletcher *et al.* [5]) have been on 90° elastic scattering from 4.4 to 30.3 eV. While most of the predictions for the spin-averaged elastic differential cross section at 90° agree with each other and with the measurements of Williams [6] and Callaway and Williams [7], as seen in Fig. 1(b), there is substantial disagreement among the same approximation methods [7–10] in the prediction of the spin asymmetry $A_{1s\text{-}1s}(90°,k^2)$, as seen in Fig. 1(a). From 10 to 30 eV, the experimental values for $A_{1s\text{-}1s}(90°,k^2)$ agree only with the prediction of $1s2s2p$ three-state close-coupling calculations (Burke and Schey [8], Burke, Schey, and Smith [9]), while the sophisticated algebraic variational pseudo-state close-coupling (CC) method [7], which provides the closest agreement with the experiments on differential cross sections, fails to predict the correct qualitative shape of the experimental profile for the parameter $A_{1s\text{-}1s}(90°,k^2)$. Another important feature which Fletcher *et al.* [5] failed to report is the distinct resonant structure shown by the three-state CC calculation [8,9] on the $A_{1s\text{-}1s}(\theta,k^2)$ parameter at energies just below the $n=2$ excitation threshold. The above-mentioned findings lead to conjectures that (i) close-coupling calculations which include only physical atomic states are more effective in describing the short-range spin-exchange interaction; (ii) the $A_{1s\text{-}1s}(\theta,k^2)$ parameter may be more sensitive to the resonant effects than the spin-averaged elastic differential cross sections.

Warner, Rutter, and King [11] reported high-energy resolution spectra of electrons scattered elastically from atomic hydrogen over the energies ranging 0.68–0.76 Ry and at angles 33°, 54°, 70°, and 90°. The positions and widths for the resonances $^1S^e$, $^3P^o$, and $^1D^e$ were extracted from the resonant profiles. The observed resonant positions were reported to be in excellent agreement with the theoretical energies of Taylor and Burke [12]. However, the agreement between the corresponding resonant widths is not so good. To resolve the discrepancy, it may be more meaningful to have the resonant profile on elastic differential cross sections reproduced theoretically and match directly with the experiments, or alternatively, it would be constructive to carry out another theoretical reconfirmation on the widths and positions of the resonances using the $A_{1s\text{-}1s}(\theta,k^2)$ parameter as a gauge if the $A_{1s\text{-}1s}(\theta,k^2)$ parameter is as sensitive to resonances as we would have expected.

In this paper, the 15-state R-matrix calculations of Pathak and co-workers [13,14] have been extended to calculate the elastic differential cross sections and the spin asymmetry in the elastic scattering of spin-polarized electrons by spin-polarized atoms. The aims of this paper are (i) to probe the sensitivity of the $A_{1s\text{-}1s}(\theta,k^2)$ parameter in response to the presence of resonances; (ii) to reconfirm the observation of resonances reported by Warner, Rutter, and King [11]; (iii) to carry out convergence studies on the close-coupling expansion in the calculation of elastic differential cross sections and the spin asymmetry.

II. THE CALCULATION

The R-matrix method for electron-atom collisions has been discussed in detail (see Burke, Hibbert, and Robb [15] and Berrington *et al.* [16]). The target wave functions, energy levels, and scattering wave functions used in the present 15-state R-matrix calculation have been fully described by Pathak, Kingston, and Berrington [13] and Aggarwal *et al.* [17]. However, to recapitulate, the wave function describing the two-electron scattering system can be expanded as

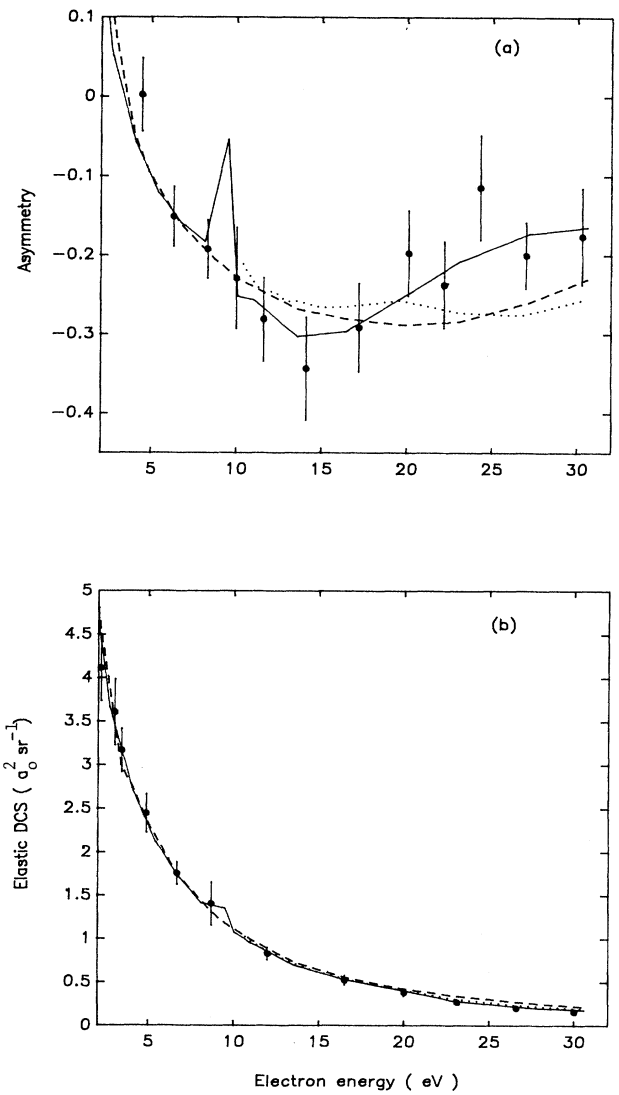

FIG. 1. Variation of (a) the $A_{1s\text{-}1s}(90°,k^2)$ parameter; (b) elastic differential cross sections at an angle of 90° as functions of incident electron energy (in eV). (a) ——, the three-state CC approximation [8,9]; – – – –, the $1s$-$2\bar{p}$ pseudo-state calculation of Fon, Burke, and Kingston [10]; ·····, the algebraic variational pseudo-state close-coupling [7]; ●, the experiments of Fletcher *et al.* [5]. (b) Same as (a) except the experiments belong to Callaway and Williams [7] and Williams [6].

$$\psi_k = \sum_{i,j} a_{ijk}\,\Phi_i u_j(r) + \sum_j b_{jk}\phi_j \ , \tag{1}$$

where Φ_i are the channel functions formed from the target states of the hydrogen atom, u_j are the radial basis functions describing the motion of the scattered electron (the continuum orbitals), and ϕ_j are the two-electron functions (the bound-bound orbitals) which allow for short-range correlation effects. These bound-bound orbitals are also designed to represent the target states of the singly ionized atom, coupled to two bounded electrons simulating the possible formation of two-electron resonances.

In theory, if the summation in (1) included all the bound states of hydrogen exactly and also included an integration over the continuum states of hydrogen then the results would be exact. However, in practice we can only include a small number of target states in (1). In this calculation, only the fifteen lowest atomic states ($n=1$, 2, 3, 4, and 5) were used in the summation (1) and we do not allow for ionization channels. The R-matrix boundary radius was taken to be 83 a.u. and 48 continuum orbitals were used for each channel-angular momentum. At energies <0.75 Ry, the calculations were limited to partial waves with angular momentum from $L=0$ to 9 only. At energies >0.75 Ry, a few more higher partial waves were needed to ensure convergence. The T-matrix elements from these higher partial waves were obtained by extrapolation and by using a simple expression derived from partial-wave Born approximation:

$$\tan\delta_L = \frac{\pi\alpha k^2}{(2L+3)(2L+1)(2L-1)} \ , \tag{2}$$

where α is the dipole polarizability of the ground-state hydrogen, while k^2 is the energy.

The detailed theory connecting the various parameters involved (such as asymmetry and polarization) in the general case, as established by Burke and Schey [8] and Kleinpoppen [18], has given the results we use for atomic hydrogen. An up-to-date survey will be found in the recent reviews by Hanne [19] and Kessler [20]. The asymmetry is defined as the difference in the cross sections for spin-parallel and spin-antiparallel scattering, for a specific transition, normalized by the sum of the cross sections. For i to j transition

$$A_{ij}(\theta,k_i^2) = \frac{\sigma_{ij}(\uparrow\downarrow)-\sigma_{ij}(\uparrow\uparrow)}{\sigma_{ij}(\uparrow\downarrow)+\sigma_{ij}(\uparrow\uparrow)} \ , \tag{3}$$

where $\sigma_{ij}(\uparrow\downarrow)$ is the differential cross section for the process when the spins are antiparallel, $\sigma_{ij}(\uparrow\uparrow)$ is the differential cross section when the spins are parallel, while k_i^2 is the energy in the initial channel (in rydbergs). In terms of the direct $f_{ij}(\theta,k_i^2)$ and exchange $g_{ij}(\theta,k_i^2)$ amplitudes we have

$$\sigma_{ij}(\uparrow\downarrow) = |f_{ij}|^2 + |g_{ij}|^2 \ , \tag{4}$$

$$\sigma_{ij}(\uparrow\uparrow) = |f_{ij} - g_{ij}|^2 \ , \tag{5}$$

where we have suppressed the energy and angular dependence.

The ratio r_{ij} of triplet to singlet cross sections for the

transition $i \rightarrow j$ is

$$r_{ij}=\sigma_{ij}(s=1)/\sigma_{ij}(s=0) \tag{6}$$

so that the spin asymmetry can be written as

$$A_{ij}(\theta,k_i^2)=(1-r_{ij})/(1+3r_{ij}) . \tag{7}$$

Alternatively we can write

$$A_{ij}(\theta,k_i^2)=\frac{\sigma(s=0)-\sigma(s=1)}{\sigma(s=0)+3\sigma(s=1)} , \tag{8}$$

where $\frac{1}{4}\sigma(s=0)$ is the spin-weighted contribution from singlet scattering to the total differential cross section and $\frac{3}{4}\sigma(s=1)$ is the corresponding triplet cross section.

III. RESULTS AND DISCUSSIONS

The 15-state R-matrix calculations of Pathak and coworkers [13,14] and Fon, Aggarwal, and Ratnavelu [21] have been extended to obtain the differential cross sections and the spin asymmetry $A_{1s\text{-}1s}(\theta,k^2)$ for the transition

$$e^- + \mathrm{H}(1s) \rightarrow e^- + \mathrm{H}(1s) \tag{9}$$

at 685 energies ranging from 1 to 17 eV in order to depict the detailed resonant structures of the observed profile on the elastic differential cross sections and the $A_{1s\text{-}1s}(\theta,k^2)$ parameter as functions of electron energies. The calculations are computed at scattering angles of 30°, 55°, 70°, and 90°. To check the accuracy and consistency of the calculations, the elastic differential cross sections and the $A_{1s\text{-}1s}(\theta,k^2)$ parameter are also presented as functions of scattering angle at a few energies (see Tables I and II and Figs. 6–9).

A complete presentation of all the results of these calculations would require publication of a very large table giving the cross sections and the values of $A_{1s\text{-}1s}(\theta,k^2)$ as functions of 685 energies. This is impractical. Therefore, it has been decided to present here some illustrative results in graphical form. A numerical table of the results by energies at 30°, 55°, 70°, and 90° can be obtained on request from the authors [22].

A. Elastic differential cross sections and the $A_{1s-1s}(90°,k^2)$ parameter as functions of energies

Figure 2 compares the three-state CC approximation [8,9] and the 15-state R-matrix calculation on elastic differential cross sections and $A_{1s\text{-}1s}(90°,k^2)$ with the ex-

TABLE I. The 15-state R-matrix calculation of the elastic differential cross section in units of a_0^2 sr^{-1}. (Figures in brackets denote the power of 10 by which the number should be multiplied.)

Angle (deg) \ k^2	0.81 Ry	0.8823 Ry	1.00 Ry	1.21 Ry
0	7.946	7.962	8.190	8.240
5	6.949	6.978	7.022	6.952
10	6.033	6.024	5.958	5.784
15	5.292	5.249	5.106	4.855
20	4.669	4.592	4.392	4.086
25	4.120	4.014	3.776	3.429
30	3.624	3.495	3.238	2.865
35	3.178	3.031	2.770	2.385
40	2.784	2.626	2.370	1.987
45	2.442	2.278	2.033	1.663
50	2.150	1.984	1.754	1.403
55	1.901	1.735	1.522	1.197
60	1.688	1.526	1.330	1.031
65	1.506	1.349	1.170	8.958 [−1]
70	1.350	1.200	1.037	7.853 [−1]
75	1.219	1.076	9.261 [−1]	6.952 [−1]
80	1.110	9.745 [−1]	8.357 [−1]	6.228 [−1]
85	1.023	8.931 [−1]	7.628 [−1]	5.652 [−1]
90	9.528 [−1]	8.292 [−1]	7.047 [−1]	5.196 [−1]
100	8.603 [−1]	7.448 [−1]	6.238 [−1]	4.548 [−1]
110	8.218 [−1]	7.074 [−1]	5.802 [−1]	4.152 [−1]
120	8.282 [−1]	7.074 [−1]	5.655 [−1]	3.935 [−1]
130	9.663 [−1]	7.321 [−1]	5.700 [−1]	3.821 [−1]
140	9.234 [−1]	7.705 [−1]	5.868 [−1]	3.775 [−1]
150	9.896 [−1]	8.162 [−1]	6.110 [−1]	3.788 [−1]
160	1.051	8.602 [−1]	6.349 [−1]	3.820 [−1]
170	1.094	8.911 [−1]	6.495 [−1]	3.823 [−1]
180	1.109	9.015 [−1]	6.534 [−1]	3.813 [−1]

periments (Williams [6], Callaway and Williams [7], and Fletcher *et al.* [5]). In Fig. 2(a), it is observed that both calculations lie well within the experimental limits of the measurements on the spin asymmetry $A_{1s\text{-}1s}(90°,k^2)$ over the entire energy range from 6 to 15 eV. The 15-state R-matrix calculation on $A_{1s\text{-}1s}(90°,k^2)$ exhibits distinct resonant structures at the neighborhood of the $n=2$ excitation threshold. The indication of resonant characteristic is also shown by the three-state CC calculation [8,9] which would have echoed with a similar resonant profile if calculations were to be carried out at more energy points. The resonances with broad widths $^1S^e$ and $^1D^e$ are clearly shown at the positions 9.557 and 10.126 eV. In Fig. 2(b), the elastic differential cross section represented as a function of energy reflects similar resonant structures at the vicinity of the $n=2$ excitation threshold in confirmation of the observation of these resonances.

In Fig. 2(a), the 15-state R-matrix calculation on $A_{1s\text{-}1s}(90°,k^2)$ indicates significant resonant structures at $n=3$ and 4 excitation thresholds. Similar resonant features (although in a very much reduced magnitude) are also weakly reflected in Fig. 2(b) by the 15-state R-matrix calculation of elastic differential cross sections. To identify the resonances lying below and converging on the $n=3$ hydrogen threshold, we magnify the profiles of the 15-state R-matrix calculation, over the energies ranging from 0.85 to 0.9 Ry, on the spin asymmetry $A_{1s\text{-}1s}(90°,k^2)$ in Fig. 3(a) and the elastic differential cross sections in Fig. 3(b). Again, the qualitative shape of the two curves shows remarkable resemblance to each other. Resonances $^1S^e$, $^1D^e$, $^1S^e$, $^1D^e$, and $^1G^e$ which have widths greater than 4.0×10^{-4} Ry are predicted by both curves at 0.8620, 0.8681, 0.8845, 0.8864, and 0.8875 Ry. The absence of the P-wave resonances is noted.

B. Elastic differential cross sections and the $A_{1s-1s}(\theta,k^2)$ parameter at scattering angles other than 90°

Figures 4 and 5 compare the profiles of the 15-state R-matrix calculations for the $A_{1s\text{-}1s}(\theta,k^2)$ parameter with those of the elastic differential cross sections obtained from the same R-matrix calculation and the experimental yield on the measurement of the elastic cross sections at scattering angles of 30°, 55°, 70°, and 90° performed by Warner, Rutter, and King [11]. The following features are observed: (i) in all cases considered here, the $A_{1s\text{-}1s}(\theta,k^2)$ parameter as a function of energy exhibits

TABLE II. The 15-state R-matrix calculation on the spin asymmetry $A_{1s\text{-}1s}(\theta,k^2)$. (Figures in brackets denote the power of 10 by which the number should be multiplied.)

Angle (deg) \ k^2	0.81 Ry	0.8823 Ry	1.00 Ry	1.21 Ry
0	−1.89 [−1]	−1.82 [−1]	−1.80 [−1]	−1.61 [−1]
5	−2.02 [−1]	−1.93 [−1]	−1.93 [−1]	−1.72 [−1]
10	−2.15 [−1]	−2.06 [−1]	−2.06 [−1]	−1.84 [−1]
15	−2.26 [−1]	−2.17 [−1]	−2.17 [−1]	−1.95 [−1]
20	−2.35 [−1]	−2.27 [−1]	−2.27 [−1]	−2.07 [−1]
25	−2.44 [−1]	−2.36 [−1]	−2.37 [−1]	−2.19 [−1]
30	−2.51 [−1]	−2.45 [−1]	−2.46 [−1]	−2.31 [−1]
35	−2.58 [−1]	−2.53 [−1]	−2.55 [−1]	−2.44 [−1]
40	−2.64 [−1]	−2.61 [−1]	−2.63 [−1]	−2.56 [−1]
45	−2.69 [−1]	−2.68 [−1]	−2.70 [−1]	−2.68 [−1]
50	−2.73 [−1]	−2.75 [−1]	−2.77 [−1]	−2.80 [−1]
55	−2.76 [−1]	−2.80 [−1]	−2.82 [−1]	−2.89 [−1]
60	−2.78 [−1]	−2.84 [−1]	−2.87 [−1]	−2.98 [−1]
65	−2.79 [−1]	−2.88 [−1]	−2.90 [−1]	−3.05 [−1]
70	−2.78 [−1]	−2.90 [−1]	−2.92 [−1]	−3.10 [−1]
75	−2.77 [−1]	−2.90 [−1]	−2.93 [−1]	−3.14 [−1]
80	−2.74 [−1]	−2.89 [−1]	−2.92 [−1]	−3.15 [−1]
85	−2.69 [−1]	−2.85 [−1]	−2.88 [−1]	−3.13 [−1]
90	−2.62 [−1]	−2.78 [−1]	−2.81 [−1]	−3.07 [−1]
100	−2.37 [−1]	−2.54 [−1]	−2.55 [−1]	−2.83 [−1]
110	−1.99 [−1]	−2.15 [−1]	−2.15 [−1]	−2.42 [−1]
120	−1.55 [−1]	−1.68 [−1]	−1.66 [−1]	−1.85 [−1]
130	−1.06 [−1]	−1.15 [−1]	−1.12 [−1]	−1.13 [−1]
140	−6.13 [−2]	−6.26 [−2]	−6.01 [−2]	−3.73 [−2]
150	−2.67 [−2]	−2.12 [−2]	−2.01 [−2]	2.67 [−2]
160	−4.23 [−3]	6.05 [−3]	7.61 [−3]	7.60 [−2]
170	8.81 [−3]	2.19 [−2]	2.78 [−2]	1.15 [−1]
180	1.36 [−2]	2.78 [−2]	3.70 [−2]	1.32]−1]

rapid variation in the close vicinity of the resonances; (ii) only at scattering angle 90° as seen in Figs. 4(d) and 4(e), the qualitative shape of the profiles belonging to the $A_{1s\text{-}1s}(\theta,k^2)$ parameter and elastic differential cross sections shows remarkable resemblance to each other. However, this resemblance is not carried over to other angles at 30°, 55°, and 70°; (iii) the 15-state R-matrix calculation on the cross section reproduces the detailed profile of the experimental measurements made by Warner, Rutter, and King [11] at scattering angles 30°, 55°, 70°, and 90°. At 90°, the P-wave resonances are suppressed and only the $^1S^e$ and $^1D^e$ resonances of broad widths are observed at 0.7024 and 0.7442 Ry on both the experimental and theoretical curves. At 55°, the $^1D^e$ resonance at 0.7442 Ry is suppressed and only the $^1S^e$ and $^3P^o$ resonances show up at 0.7024 and 0.7159 Ry on the cross-section profile; (iv) the calculated profiles of $A_{1s\text{-}1s}(\theta,k^2)$ at scattering angles of 30°, 55°, and 70° predict correctly all the three resonances $^1S^e$, $^3P^o$, and $^1D^e$ at 0.7024, 0.7159, and 0.7442 Ry without discrimination. The experimental observation of these resonances reported by Warner, Rutter, and King [11] is reconfirmed.

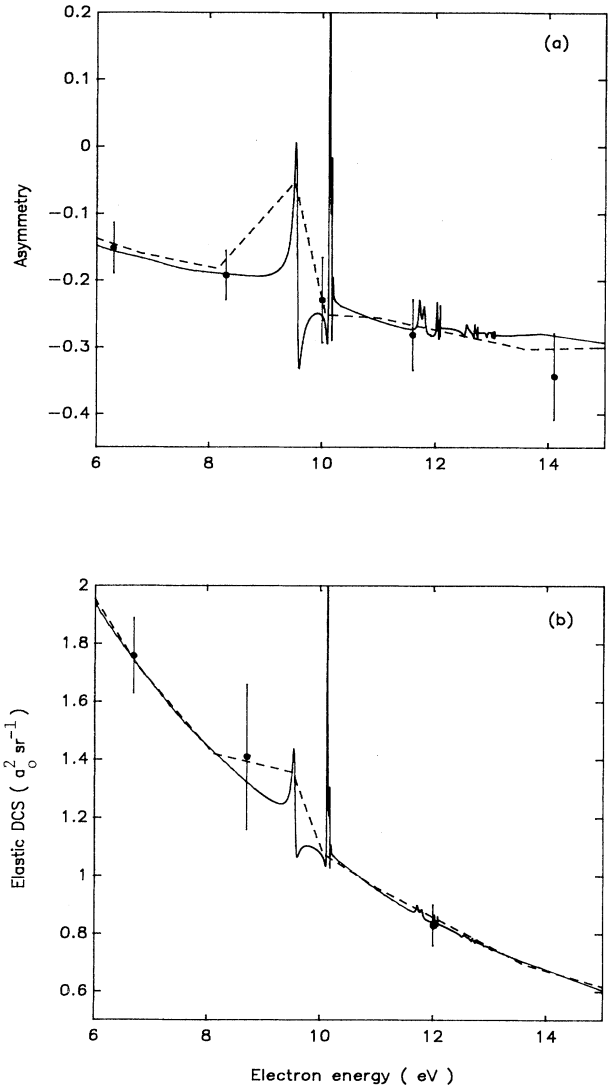

FIG. 2. Variation of (a) the $A_{1s\text{-}1s}(90°,k^2)$ parameter; (b) elastic differential cross sections at a scattering angle of 90° as functions of incident electron energy (in eV). (a) ——, the 15-state R-matrix calculation; — — —, the $1s2s2p$ three-state CC calculation [8,9]; ●, the experiments of Fletcher *et al.* [5]. (b) Same as (a) except the experiments belong to Callaway and Williams [7] and Williams [6].

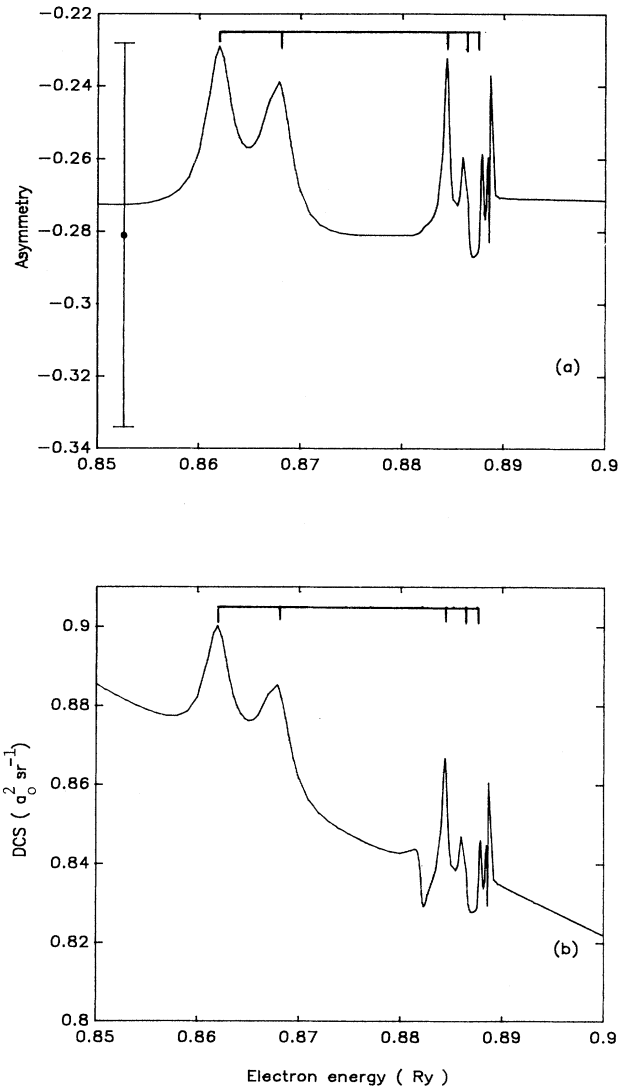

FIG. 3. Variation of (a) the $A_{1s\text{-}1s}(90°,k^2)$ parameter; (b) elastic differential cross sections at a scattering angle of 90° as functions of incident electron energy (in Ry). The legend for the data is the same as in Fig. 2. Resonances $^1S^e$, $^1D^e$, $^1S^e$, $^1D^e$, and $^1G^e$ with widths greater than 4.0×10^{-4} Ry are indicated at positions with increasing energies 0.8620, 0.8681, 0.8845, 0.8864, and 0.8875 Ry.

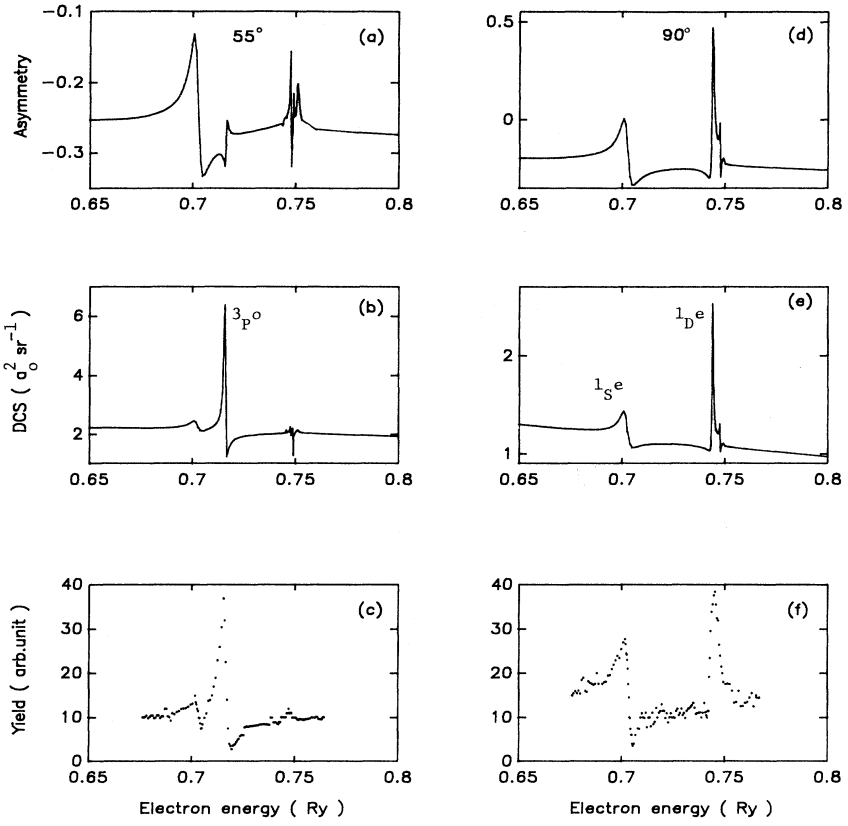

FIG. 4. Variation of the $A_{1s\text{-}1s}(\theta,k^2)$ parameter and elastic differential cross sections as functions of incident electron energy at fixed angles. (a), (d) 15-state R-matrix calculation on $A_{1s\text{-}1s}(\theta,k^2)$ at 55° and 90°; (b), (e) 15-state R-matrix calculation on elastic differential cross sections at 55° and 90°; (c), (f) experimental measurements on elastic differential cross sections by Warner, Rutter, and King [11] at 54° and 90°.

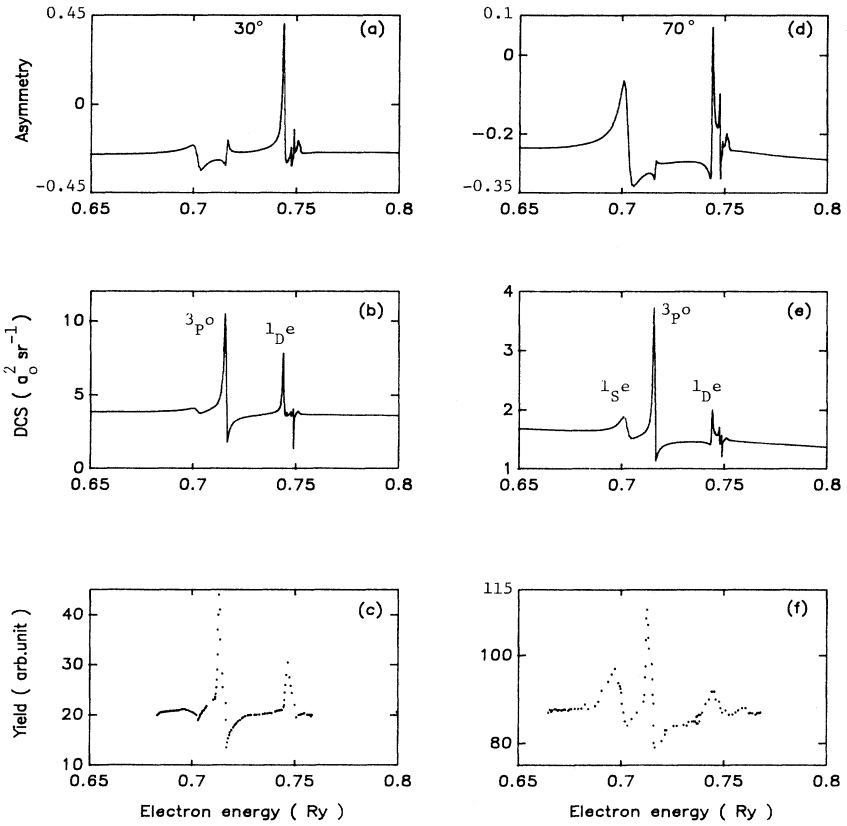

FIG. 5. Variation of the $A_{1s\text{-}1s}(\theta,k^2)$ parameter and elastic differential cross sections as functions of incident electron energy (in Ry) at a fixed angle. The legend for the data is the same as in Fig. 4 except the electron scattering angles are now 30° and 70°.

C. Elastic differential cross section and the spin asymmetry $A_{1s-1s}(\theta,k^2)$ expressed as functions of scattering angles at a fixed energy

In Figs. 6 and 7, the spin asymmetry and elastic differential cross section are expressed as functions of scattering angles at a fixed energy. In order to examine the general behavior of the profiles, calculations are carried out at energies ranging from 0.1 to 0.81 Ry.

Figure 6 compares the calculation of $A_{1s\text{-}1s}(\theta,k^2)$ parameter obtained from the three-state CC method [8,9] with those derived from the 15-state R-matrix calculation. The general profiles for the $A_{1s\text{-}1s}(\theta,k^2)$ obtained from both methods show the development of a minimum starting from 20° at 0.3 Ry as seen in Fig. 6(e) and the position of the minimum slowly shifts to larger angle 65° at 0.81 Ry [see Fig. 6(a)]. Except at $k^2=0.7$ Ry, the profile of the $A_{1s\text{-}1s}(\theta,k^2)$ deviates from the general pattern. This unusual behavior is attributed to the presence of a $^1S^e$ resonance at 0.7024 Ry.

At energies $k^2=1.0$ Ry, the minimum of $A_{1s\text{-}1s}(\theta,k^2)$ obtained from the three-state CC method [8,9] reaches as far as the angle 85°. As energy increases further, the position of this minimum of $A_{1s\text{-}1s}(\theta,k^2)$ slowly shifts back to a smaller angle. It is the turning around property of the minimum of $A_{1s\text{-}1s}(\theta,k^2)$ which causes the value of $A_{1s\text{-}1s}(90°,k^2)$ to rise up over the energies ranging from 1.0 to 2.25 Ry and is instrumental to the subsequent agreement between the three-state CC calculation [8,9] and the measurement of Fletcher *et al.* [5] as shown in Fig. 1(a). This turning around property in this energy range is not obvious in the calculations which include pseudo-states in the close-coupling expansion (e.g., Callaway and Williams [7] and Fon *et al.* [23]).

Another interesting feature observed in the comparison between the three-state CC approximation [8,9] and the 15-state R-matrix calculation on the spin asymmetry (see Fig. 6) and the elastic differential cross sections (see Fig. 7) is that they are in remarkably good agreement with each other especially in the case of elastic cross section. Remarkable in the sense that they are both formulated in the close-coupling framework; the three-state CC calculation [8,9] is a simple calculation which includes only 1s, 2s, and 2p orbitals, while the 15-state R-matrix calculation includes 15 target orbitals ($n=1$, 2, 3, 4, and 5) in the close-coupling expansion. The close agreement be-

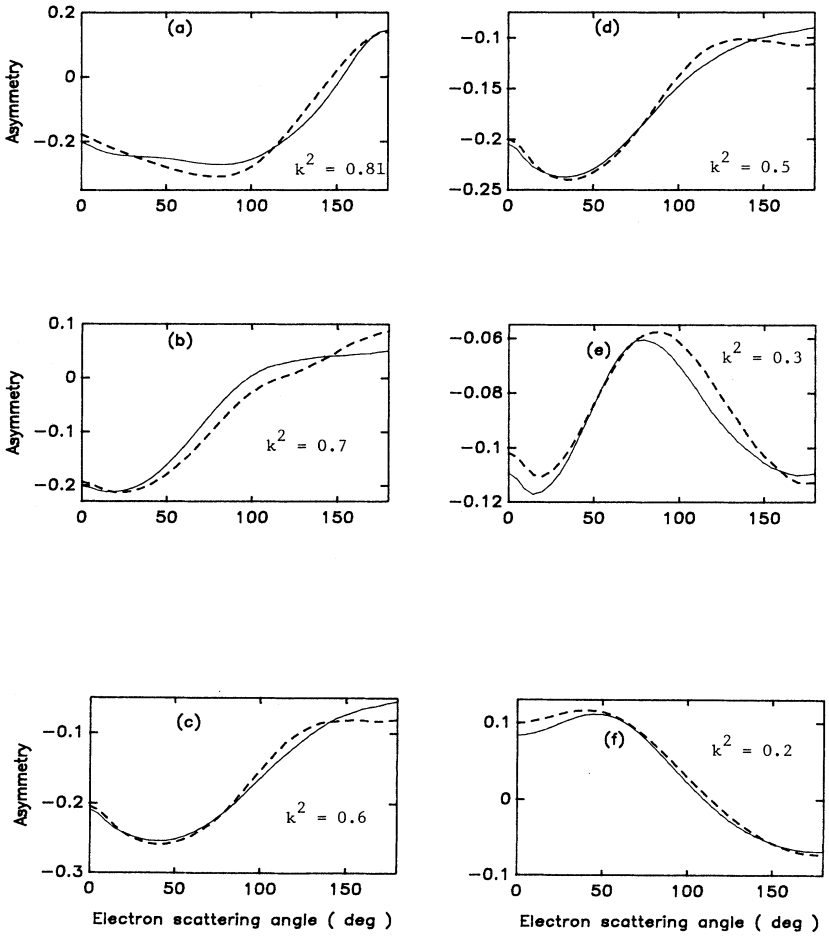

FIG. 6. Variation of the $A_{1s\text{-}1s}(\theta,k^2)$ parameter as a function of electron scattering angle (in deg) at energies (in Ry). (a) 0.81, (b) 0.7, (c) 0.6, (d) 0.5, (e) 0.3, and (f) 0.2. ——, the 15-state R-matrix calculation; — — —, the three-state CC approximation [8,9].

tween the two calculations can be interpreted as either that the three-state CC approximation [8,9] has already achieved convergence, or that the addition of many extra states of successively higher principal number in the close-coupling expansion on the calculation of the elastic differential cross section and the spin asymmetry is ineffective and the convergence is slow.

D. Convergence of the close-coupling expansion

Figure 8(a) compares the three-state CC approximation [8,9] and the 15-state R-matrix calculation on the elastic differential cross sections at 1.21 Ry with the calculations by Callaway and Williams [7] and Fon *et al.* [23], and the measurements of Callaway and Williams [7]. Although the 15-state R-matrix calculation lies within the confidence limits at every experimental point, it lies noticeably lower than other theories at small scattering angles. The three-state CC approximation [8,9] underestimates considerably the experiments in the forward direction. However, at angles $\geq 40°$, the three-state CC calculation [8,9] in agreement with the 15-state R-matrix result are well within the experimental limits of Callaway and Williams [7]. Figure 8(b) projects a similar picture

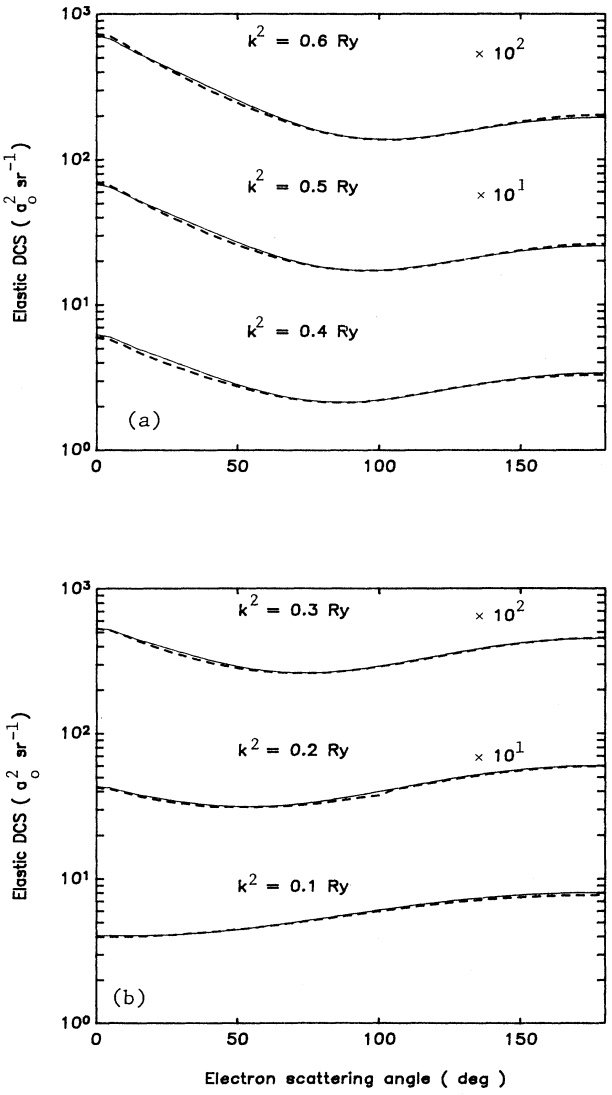

FIG. 7. Variation of elastic differential cross sections as a function of electron scattering angle (in deg). (a) At energies 0.6, 0.5, and 0.4 Ry; (b) at energies 0.3, 0.2, and 0.1 Ry. ——, the 15-state R-matrix calculation; — — —, the three-state CC approximation [8,9].

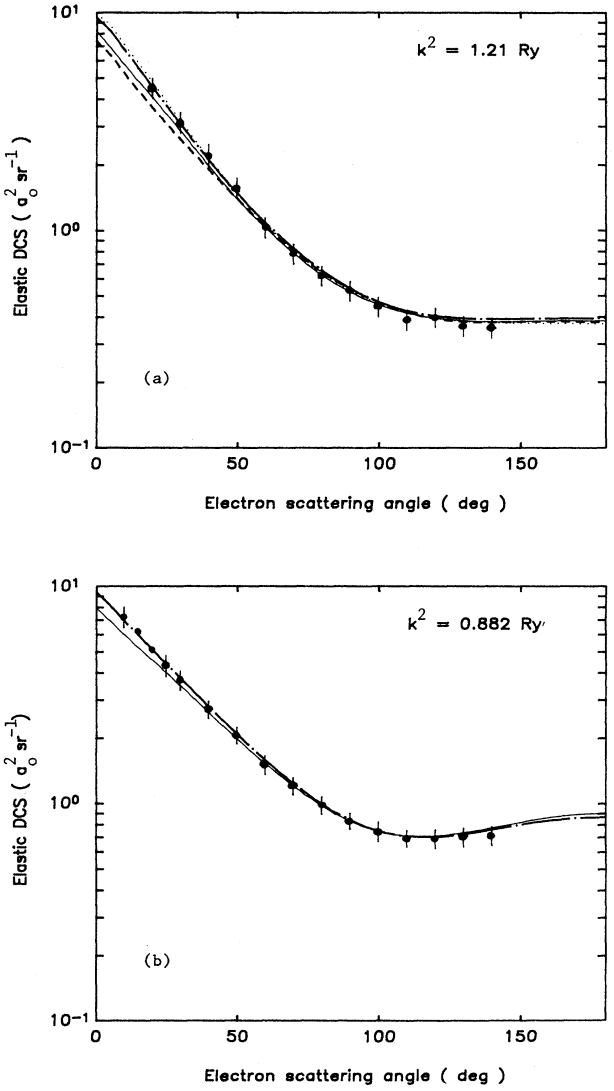

FIG. 8. Variation of elastic differential cross sections as a function of electron scattering angle (in deg) at energies. (a) 16.51 eV (k^2=1.21 Ry); (b) 12 eV (k^2=0.8823 Ry). ——, the 15-state R-matrix calculation; – – – – –, the three-state CC approximation [8,9]; —·—·—·, the algebraic variational pseudo-state close-coupling method [7]; ·····, the nine-state R-matrix calculation with pseudo-states [23]; ●, the experiments of Callaway and Williams [7].

for the 15-state R-matrix calculation at 0.8823 Ry showing deviation from the experiments in the forward direction. As the impact electron energy decreases, the underestimation of the experiments by the 15-state R-matrix calculation becomes more and more noticeable at the forward direction.

An electron incident on an atom in a nondegenerate-wave S ground state moves in a potential which has the asymptotic form

$$V(r) \underset{r\to\infty}{\sim} -\frac{\alpha}{2r^4}, \tag{10}$$

in atomic units, where α is the dipole polarizability. In the close-coupling approximation, the three-state CC calculation [8,9] accounts for only 66% of the ground-state dipole polarizability while 81.4% of α for atomic hydrogen comes from the discrete spectrum. The omission of the continuum states from the close-coupling expansion is responsible for underestimation of the elastic differential cross section in the forward direction. This explains the fact that the three-state CC approximation [8,9] and the 15-state R-matrix calculation on the elastic cross section underestimate the experimental values at small angles.

The excellent agreement obtained by the three-state CC approximation [8,9] and the 15-state R-matrix calculation with the experimental measurements on elastic cross sections at angles $\geq 40°$ indicates that the three-state CC approximation [8,9] is essentially adequate to describe the short-range interaction which affects mainly the scattering at larger angles. The 15-state R-matrix calculation on elastic cross sections is therefore to be expected to be close to the three-state CC approximation [8,9] at this angular range.

Figure 9 compares the present calculation of the spin asymmetry $A_{1s\text{-}1s}(\theta,k^2)$ with those of the three-state CC approximation [8,9], the algebraic variational pseudo-state close-coupling method [7], and the nine-state R-matrix calculation of Fon *et al.* [23]. The following facts are observed: (i) The close agreement between the calculations on elastic differential cross sections as seen in Fig. 8(a) is not reflected here in the comparison of the calculations on the $A_{1s\text{-}1s}(\theta,k^2)$ parameter by the same theoretical methods. The substantial differences between the calculated values on $A_{1s\text{-}1s}(\theta,k^2)$ parameter indicate that the demand for an accurate description of short-range forces by the calculation of the $A_{1s\text{-}1s}(\theta,k^2)$ parameter is even more stringent than that required for the calculation of spin-averaged elastic differential cross section. (ii) The calculations are divided into two mutually exclusive sets: (a) the nine-state R-matrix calculation [23] with the coupling of the pseudo-states agrees very well with the algebraic variational pseudo-state close-coupling method of Callaway and Williams [7]; (b) the present 15-state R-matrix calculation which includes only the physical target states of atomic hydrogen is in good accord with the three-state CC approximation [8,9]. Judging from the good agreement between the three-state CC calculation [8,9] and the measurement of Fletcher *et al.* [5] for the values of $A_{1s\text{-}1s}(90°,k^2)$ as shown in Fig. 1(a), it may be construed that spin exchange takes place when the incident electron and the atomic electron are in close encounter where short-range forces predominate. The distortion of the exchange force arising from the coupling of pseudo-states does not seem to predict correctly the experimental values of the spin asymmetry.

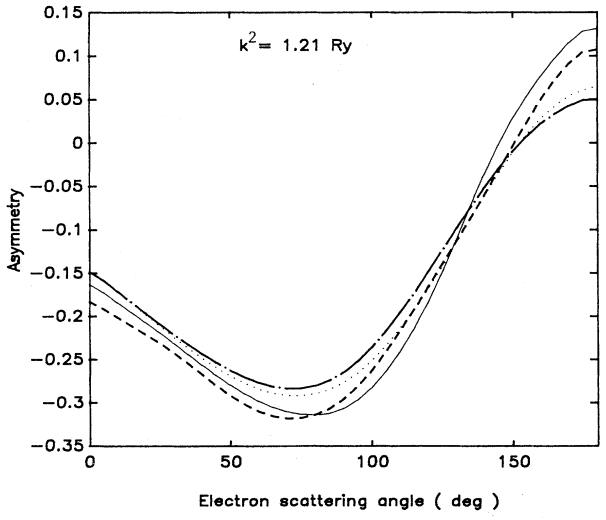

FIG. 9. The spin asymmetry $A_{1s\text{-}1s}(\theta,k^2)$ as a function of scattering angle (in deg) at energy 16.51 eV ($k^2=1.21$ Ry). The legend for the data is the same as in Fig. 8.

IV. CONCLUSION

A 15-state R-matrix calculation on elastic differential cross sections and spin asymmetry have been carried out at 685 energies and over a wide range of angles. We are satisfied with the following conclusions: (i) the $A_{1s\text{-}1s}(\theta,k^2)$ parameter is more sensitive to the presence of resonances than the spin-averaged elastic differential cross sections; (ii) the 15-state R-matrix calculations on elastic differential cross sections in agreement with the three-state CC approximation predict correctly the experimental values measured by Callaway and Williams [7] except at small scattering angles where the underestimation is attributed to their inability in calculating the ground-state dipole polarizability correctly by not including continuum-states into the close-coupling expansion. However, we have sufficient evidences to suggest that the calculation on the spin asymmetry by the 15-state R-matrix method in which only physical atomic states are included in the close-coupling expansion is essentially correct. Further experiments and theoretical calculations are needed to verify this.

ACKNOWLEDGMENTS

We would like to thank Professor P. G. Burke FRS, Professor A. E. Kingston, Dr. A. Pathak, and Dr. K. A. Berrington for their continued interest and support. The

majority of these calculations were carried out on the CRAY X-MP/48 computer at the SERC Atlas Laboratory, Didcot, United Kingdom. Data analysis was carried out on the UNISYS 1100/61 computer systems at the Computer Centre, University of Malaya, Kuala Lumpur. F.W.C. and K.R. would also like to acknowledge financial assistance from University of Malaya Research Funds (Vote F).

---

*Permanent address: Department of Physics and Astrophysics, University of Delhi, Delhi 110007, India.

[1] M. J. Alguard, V. W. Hughes, M. S. Lubell, and P. F. Wainwright, Phys. Rev. Lett. **39**, 334 (1977).
[2] P. F. Wainwright, M. J. Alguard, G. Baum, and M. S. Lubell, Rev. Sci. Instrum. **44**, 571 (1978).
[3] G. D. Fletcher, M. J. Alguard, T. J. Gay, V. W. Hughes, C. D. Tu, P. F. Wainwright, M. S. Lubell, W. Raith, and F. C. Tang, Phys. Rev. Lett. **48**, 1671 (1982).
[4] T. J. Gay, G. D. Fletcher, M. J. Alguard, V. W. Hughes, P. F. Wainwright, and M. S. Lubell, Phys. Rev. A **26**, 3664 (1982).
[5] G. D. Fletcher, M. J. Alguard, T. J. Gay, V. W. Hughes, P. F. Wainwright, M. S. Lubell, and W. Raith, Phys. Rev. A **31**, 2854 (1985).
[6] J. F. Williams, J. Phys. B **8**, 1683 (1975).
[7] J. Callaway and J. F. Williams, Phys. Rev. A **12**, 2312 (1975).
[8] P. G. Burke and H. M. Schey, Phys. Rev. **126**, 147 (1962).
[9] P. G. Burke, H. M. Schey, and K. Smith, Phys. Rev. **129**, 1258 (1963).
[10] W. C. Fon, P. G. Burke, and A. E. Kingston, J. Phys. B **11**, 521 (1978).
[11] C. D. Warner, P. M. Rutter, and G. C. King, J. Phys. B **19**, 3297 (1986).
[12] A. J. Taylor and P. G. Burke, Proc. Phys. Soc. London **92**, 336 (1967).
[13] A. Pathak, A. E. Kingston, and K. A. Berrington, J. Phys. B **21**, 2939 (1988).
[14] A. Pathak, P. G. Burke, and K. A. Berrington, J. Phys. B **22**, 2759 (1989).
[15] P. G. Burke, A. Hibbert, and W. D. Robb, J. Phys. B **4**, 153 (1971).
[16] K. A. Berrington, P. G. Burke, M. Le Dourneuf, W. D. Robb, K. T. Taylor, and Vo Ky Lan, Comput. Phys. Commun. **14**, 367 (1978).
[17] K. M. Aggarwal, K. A. Berrington, P. G. Burke, A. E. Kingston, and A. Pathak, J. Phys. B **24**, 1385 (1991).
[18] H. Kleinpoppen, Phys. Rev. A **3**, 2015 (1971).
[19] G. F. Hanne, Phys. Rep. **95**, 95 (1983).
[20] J. Kessler, *Polarized Electrons* (Springer-Verlag, Berlin, 1976).
[21] W. C. Fon, K. M. Aggarwal, and K. Ratnavelu, J. Phys. B **25**, 2625 (1992).
[22] The results can be obtained in printed form or via electronic mail at the address j2kurun@ccvax.cc.um.MY
[23] W. C. Fon, K. A. Berrington, P. G. Burke, and A. E. Kingston, J. Phys. B **14**, 1041 (1981).